Predicting visual acuity from the structure of visual cortex

Shyam Srinivasan[a,b,1], C. Nikoosh Carlo[a,1], and Charles F. Stevens[a,b,2]

[a]Molecular Neurobiology Laboratory, Salk Institute for Biological Studies, La Jolla, CA 92037; and [b]Kavli Institute for Brain and Mind, University of California, San Diego, CA 92093

Contributed by Charles F. Stevens, May 13, 2015 (sent for review November 14, 2014; reviewed by David A. Leopold and Clay Reid)

Three decades ago, Rockel et al. proposed that neuronal surface densities (number of neurons under a square millimeter of surface) of primary visual cortices (V1s) in primates is 2.5 times higher than the neuronal density of V1s in nonprimates or many other cortical regions in primates and nonprimates. This claim has remained controversial and much debated. We replicated the study of Rockel et al. with attention to modern stereological precepts and show that indeed primate V1 is 2.5 times denser (number of neurons per square millimeter) than many other cortical regions and nonprimate V1s; we also show that V2 is 1.7 times as dense. As primate V1s are denser, they have more neurons and thus more pinwheels than similar-sized nonprimate V1s, which explains why primates have better visual acuity.

visual acuity | V1 | primates | vision | pinwheels

Rockel et al. (1), in an influential and controversial article entitled "The basic uniformity in structure of the neocortex," reported that the number of neurons underneath a square millimeter of neocortical surface is constant for six cortical areas and five species with one exception: primate primary visual cortex (V1) has a surface density of about 250,000 neurons/mm^2, around two and a half times the usual density for other areas studied.

The Rockel et al. paper has, for a third of a century, continued to generate controversy for two reasons. One reason stems from its implications for an equally energetic debate among neuroscientist "lumpers" and "splitters." Cortical uniformity supports a theory of neocortical processing wherein different cortical areas are subserved by the same canonical circuit, a view favored by lumpers. Splitters, however, believe each cortical area to be different and doubt the paper's claims (2). The second reason is that studies from various laboratories using different measurement methods over the last three decades have alternately agreed and disagreed with Rockel et al.'s results (2).

Notably, however, Rockel et al's studies have never been directly replicated. We set out to repeat the observations for the same areas and species Rockel et al. used. We used Rockel et al.'s counting techniques but with attention to the precepts of modern stereology (2). Our goal was to simply determine if Rockel et al.'s observations are repeatable rather than address the larger question of numerical uniformity of neocortex across species and areas. In an earlier publication (2), we confirmed Rockel et al.'s conclusions for nonvisual areas. Here we focus on the primary V1 for the same species used in the original report of Rockel et al.

V1 is part of the visual circuit from the retina to the cortex, which is retinotopically organized, and the 2D image of the world that is mapped onto the retina is recreated in V1 (3). Cells within the retina capture visual information for each image location or pixel such as color and light intensity and convey it to structures in V1 (4, 5), which perform computations that contribute to visual abilities. An especially well-studied V1 structure is a pinwheel, which comprises orientation columns that extend vertically down from the cortical surface, containing cells with receptive fields responsive to lines or edges at a particular angle. Columns within a pinwheel are organized so that the angle of orientation increases/decreases smoothly as one radially traverses the cortical surface and stays constant as one moves along a spoke of the pinwheel (5, 6). We wondered whether evolution might have designed primate V1 to be denser to increase the number of cells and pinwheels (7) and thus the computational power of V1 and visual abilities (8).

We estimated the neuronal surface density (the number of neurons under a square millimeter of neocortical surface) of V1 for mouse, rat, cat, and monkey (rhesus macaque) and confirmed Rockel et al.'s original report: the first three species have a surface density of about 10^5 neurons/mm^2 and monkey V1 has about 2.5×10^5 neurons/mm^2. We also found that monkey V2 has about 1.7×10^5 neurons/mm^2.

Results

Rockel et al. studied six neocortical areas—frontal (Brodmann 9), motor (4), somatosensory (S1), parietal (7), primary visual (17 or V1), and temporal (22)—in the mouse, rat, cat, monkey (rhesus macaque), and human, and in addition, just the V1 in the tupaia, galago, marmoset, baboon, and chimpanzee. All these areas had close to the same neuronal surface density except for primate V1, where the surface density for all seven species Rockel et al. studied was about 2.5 times that of the other areas. We report our replication of Rockel et al.'s observations on V1, except we only had access to macaques among primates. Earlier, we reported that our observations for four areas (motor, somatosensory, parietal, and temporal) and four species (mouse, rat, cat, and monkey) confirmed those of Rockel et al. (1). We now report that our observations on V1 for the same four species confirm Rockel et al. (see *Experimental Procedures*, Table S1, and Fig. S1 for methodology and representative sections). We also examined monkey V2 and found that its surface density is intermediate between that of V1 and the other areas (about 1.7 times the usual surface density).

Significance

In 1980, a group of researchers published a study claiming that the number of neurons under a square millimeter of visual cortex is 2.5 times higher in primates than nonprimates. This claim has been debated ever since. We replicated their study using modern stereology techniques and confirmed the original conclusion. What would be the advantage of this extra surface density in the visual cortex? The extra density allows primates to have 2.5 times more neurons and computational power in their visual cortex. As a result, their visual acuity is better than their nonprimate mammalian relatives.

Author contributions: S.S., C.N.C., and C.F.S. designed research; S.S., C.N.C., and C.F.S. performed research; C.F.S. contributed new reagents/analytic tools; S.S., C.N.C., and C.F.S. analyzed data; S.S. and C.F.S. wrote the paper; and C.N.C. and C.F.S. conceived the project.

Reviewers: D.A.L., National Institute of Mental Health; and C.R., Allen Institute.

The authors declare no conflict of interest.

[1]S.S. and C.N.C. contributed equally to this work.

[2]To whom correspondence should be addressed. Email: stevens@salk.edu.

This article contains supporting information online at www.pnas.org/lookup/suppl/doi:10.1073/pnas.1509282112/-/DCSupplemental.

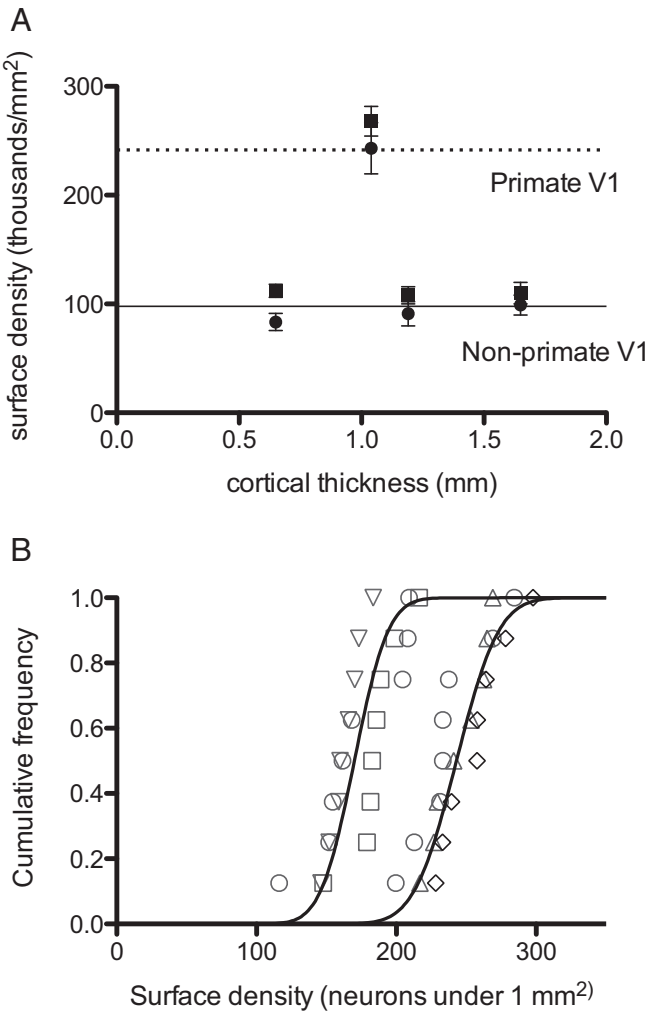

Fig. 1. Primate visual areas have higher neuronal densities than nonprimate visual areas. (*A*) Surface densities of V1 in primates (macaques: upper dotted line) and nonprimates (mouse, rat, and cat: lower solid line), with mouse, monkey, rat, and cat in increasing order of thickness. Primate V1 neuronal surface density is 2.44 times nonprimate V1 density, as shown by the clustering of primate brains on the upper (value of 244) line and nonprimates on the lower (value of 100) line. Squares represent data from the paper of Rockel et al. and circles represent data from our experiments. The cortical thickness of each species was calculated from our data. See Tables S2–S7 for values. (*B*) Cumulative histograms of surface density counts of macaque V1 and V2 with best-fit cumulative Gaussians. The mean and SD for V2 (the curve to the left) are 170 ± 19 and for V1 are 243 ± 23.5. There is no overlap in the counts for the two regions, and V1 is 1.4 times the density of V2. Each symbol denotes counts from separate columns within the same animal.

In Fig. 1*A*, Rockel et al.'s average V1 surface densities (neurons per square millimeter) for mouse, monkey, rat, and cat are plotted (as squares) as a function of cortical thickness (our average thickness values), and our corresponding densities are plotted as circles. Rockel et al.'s surface densities are a little larger but clearly similar to our values. Furthermore, for both datasets, monkey V1 (points on the upper dotted line) has a neuronal surface density that is about 2.5 times the V1 densities of the other species (see Tables S2–S7 for values).

Rockel et al. did not correct his neuronal surface densities for brain shrinkage that occurs during histology processing, which would cause his values to be larger than the true densities. Because we used frozen sections that do not require shrinkage correction (9), our densities are likely to be closer to the true values and somewhat smaller than what Rockel et al. reported. We did not try to determine whether the differences in the two datasets can be accounted for by shrinkage because we do not know what correction to use for Rockel et al.'s data and because the main conclusions—surface density is about constant across areas and species except for primate V1, which is about 2.5 times larger—should be independent of shrinkage artifacts.

Fig. 1*B* displays data on the neuronal surface density for monkey V1 and V2. These data are derived from three monkey brains, and the measurements presented in the figure were found independently by two investigators (C.N.C. and S.S.). Neuron counts for each brain were made in eight counting frames over four to eight different sections of V1 and V2. Each counting frame's surface density was calculated using its cell counts, counting frame width, and section thickness. Different symbols (circles, squares, and triangles) are used for each brain, and our measured surface densities are displayed as cumulative histograms. Best-fitting cumulative Gaussians were found for V1 and V2 cumulative histograms in Fig. 1*B*, with a mean surface density = 243,000 ± 23,500 (SD) neurons/mm^2 for V1 and 170,000 ± 19,000 neurons/mm^2 for V2. Although some scatter is evident in the different brains, the V1 surface density is about 1.4 times larger than that of V2, and there is no overlap of the histograms describing the two brain areas.

We conclude that our replication confirms Rockel et al.'s original conclusions and that the monkey V2 neuronal surface density is intermediate between that of monkey V1 and the usual density.

Discussion

Our goal in this work was to replicate Rockel et al.'s observations on the number of neurons under a square millimeter of neocortical surface for area V1 of mouse, rat, cat, and monkey and to extend the observations to include area V2. As is apparent from the data presented in Fig. 1, our observations confirm those made by Rockel et al. (1).

In an earlier publication, we presented a graph of all available stereological data in the literature (five laboratories) on the neuronal surface density in four cortical areas and four species studied by our laboratory and Rockel et al. (figure 3A in ref. 2 and open circles in Fig. 2). Although three of the five laboratories challenged Rockel et al.'s observations, the neuronal surface

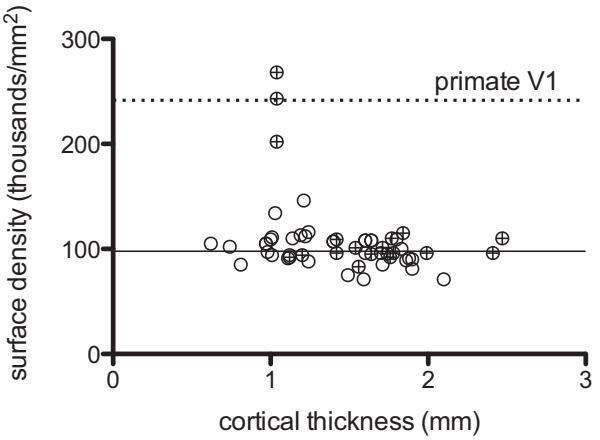

Fig. 2. Neuronal surface density of primate V1 (upper line, 241.5) is higher than neuronal densities of many other cortical areas or nonprimate V1 (lower line, 97.78). The surface density of neurons is plotted against thickness of the cortex. Circles with + symbols are density counts for primates, and open circles are density counts for nonprimates. Nonprimate density counts include data from Rockel et al., our laboratory, and the literature for V1 and non-V1 areas in four species, obtained by using stereology (see figure 3A in ref. 2 and Tables S2–S7 for values).

density across the four areas and four species is, in aggregate, essentially constant as Rockel et al. had claimed.

We are aware of only three laboratories that have measured the neuronal surface density for V1 in the species studied by Rockel et al. using stereological methods (10–14). Besides macaque, Rockel et al. reported neuronal surface densities of V1 in galago, marmoset, squirrel monkey, baboon, and chimpanzee: about 270,000 neurons under a square millimeter. Other groups have measured neuronal volume densities (number of neurons per cubic millimeter) for these species, but in the absence of cortical layer thickness estimates, deriving corresponding surface densities is not possible.

Fig. 2 presents neuronal surface densities for mouse, rat, cat, and monkey V1 from Rockel et al., our laboratory (same as Fig. 1*A*), and O'Kusky and Colonnier (12), and non-V1 areas available in the literature from five laboratories (10–14) (see Tables S2–S7 for values). Circles with + symbols are neuronal surface densities in primates, and unfilled circles are neuronal surface densities in nonprimates. The lower horizontal line in Fig. 2 is the average (97,780 neurons/mm^2 of cortical surface) of all data available from nonvisual areas (from us and other laboratories using stereology from figure 3A in ref. 2) and nonprimate V1, and the upper line is the average of all data available from primate V1 (241,500). The upper line is 2.47 times larger (the ratio of Rockel et al.'s estimates for V1 surface densities of primates to that of nonprimates). Therefore, the available comparable data support Rockel et al.'s conclusion that the neuronal surface density is approximately constant over the species and areas studied except for primate V1, which is about 2.5 (Rockel et al.'s actual estimate is 2.47) times higher.

Why Is Primate V1 Neuronal Surface Density So High? Among mammals, diurnal primates have the best vision (8). This statement is quantitated in Fig. 3*A*, where acuity (cycles per degree) is displayed as a function of V1 area (square millimeter) on a double logarithmic plot for representative diurnal haplorhines (circles with + symbols, for marmoset, squirrel monkey, crab-eating macaque, rhesus macaque, and humans in order of increasing area) and a collection of nonprimate mammals (open squares for mouse, dunnart, rat, ferret, gray squirrel, quokka, and cat, in order of increasing areas; see Tables S8 and S9 for values). V1 area for cat, sheep, and horse (crosses) was estimated from the entire neocortical area (15) by a scaling law (16) rather than direct measurements. The acuity of diurnal primates is 3- to 10-fold greater than that of nonprimate mammals with the same V1 area.

For the same reason that the upper limit on resolution of a camera is determined by the number of pixels in its photodetector array (the Nyquist sampling theorem) (17), the number of neurons in V1 sets the limit on the acuity of the visual system at V1 and beyond. Unless acuity in nonprimates is determined by some other factor (e.g., the optics of the eye or properties of the retina), primates must have more neurons in V1 than nonprimate mammals to account for the systematic differences in acuity. Primates can increase neurons by either increasing the density of neurons or keeping the density constant and increasing the V1 area or by some combination of the two. Kaskan et al. (16) compared V1 with the entire neocortex areas in 30 mammals from a variety of taxa and found that V1 areas in primates follow the same areal scaling law as nonprimates: i.e., the size of V1 in primates is not relatively larger than that of nonprimates. Thus, V1 in primates must have a higher neuronal surface density than nonprimates to explain the observed increase in primate acuity, which is exactly what Rockel et al. found.

Cells in V1 and secondary visual areas have receptive fields that respond to complex visual characteristics of objects such as speed, motion, and edge orientation (4, 18). These responses result from computations performed on retinal input (19). Computations of edge orientation by cells in V1 is an especially well-studied characteristic across species in terms of underlying anatomy and function (6, 20–23). In mammals (except for rodents), orientation selective cells are organized in the form of pinwheel structures, and these pinwheels tile the cortex in such a way that every pinwheel corresponds to a particular location of the retinal image, and as the number of pinwheels increases, the size of the retinal location they serve decreases or in other words their resolution increases (3, 7, 20, 22). For this reason, we concentrated on pinwheel structures as a proxy for V1 computations. Additionally, computations to determine edges and their orientations are relevant to tests of visual acuity (8), which have been conducted in the same species whose pinwheel organizations are well characterized.

Data from the literature show that primates have higher pinwheel densities than nonprimates (20). This finding suggests that

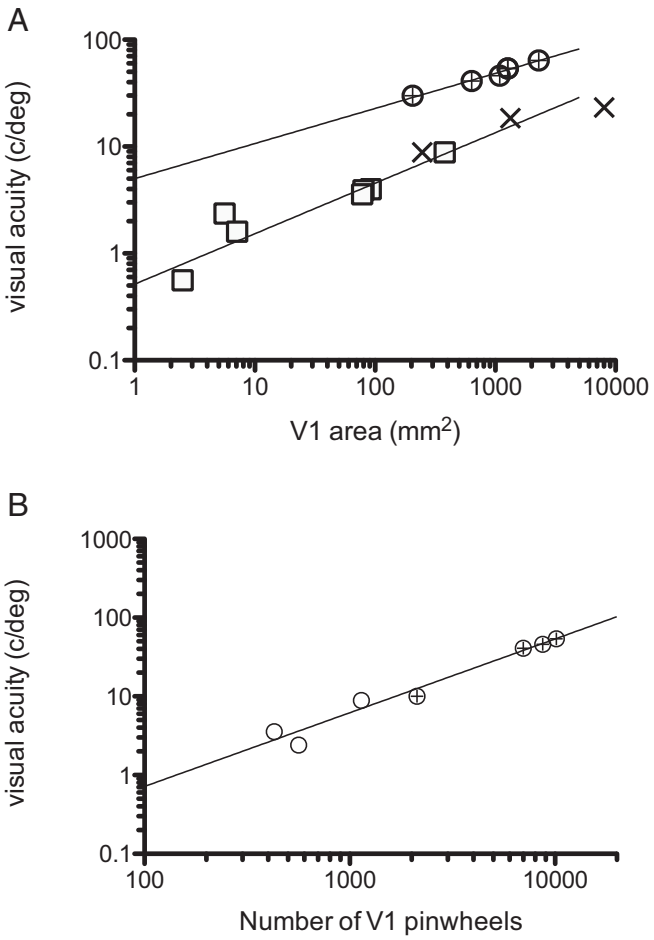

Fig. 3. Visual acuity across species increases with number of neurons and pinwheels in V1. (*A*) Log-log plot of visual acuity in cycles per degree plotted for different species (distinguished by size of V1). Circles with plus symbols denote primates (marmoset, squirrel monkey, crab-eating macaque, rhesus macaque, and humans), open squares denote nonprimates (mouse, dunnart, rat, ferret, gray squirrel, quokka, and cat), and crosses denote nonprimates (cat, sheep, and horse) whose area was estimated by using scaling laws from Kaskan et al. (16). All species are plotted in increasing order of V1 area. The primate best-fit line is given by Log A = 0.328 Log (S) + 0.7, and the nonprimate best-fit line is given by Log A = 0.472 Log (S) − 0.287, where A acuity is in cycles per degree, and S is surface area of V1 (mm^2). (*B*) Log-log plot of visual acuity vs. number of pinwheels for different species (ferret, tree shrew, cat, owl monkey, squirrel monkey, crab-eating macaque, and rhesus macaque in order of increasing pinwheels). Primates are denoted with circles containing + symbols. The best-fit line is given by Log A = 0.937 Log (N) − 2.37. N is number of pinwheels. See Tables S8 and S9 for values of A, S, and N.

primate and nonprimate pinwheels have similar properties (same number of neurons): for example, based on surface densities, the number of neurons in a cat and monkey pinwheel is roughly the same (about 33,000). If each pinwheel constitutes a pixel with about the same properties across species, primates, with a higher surface density, would have smaller pinwheels than nonprimates. This observation predicts that acuity would be proportional to pinwheel number across species. In Fig. 3*B*, acuity is plotted as a function of the total number of pinwheels for a range of species (ferret, tree shrew, cat, owl monkey, squirrel monkey, crab-eating macaque, and rhesus macaque in order of increasing number of pinwheels) and confirms this prediction.

Is Primate V1 Special? The argument above says that V1 is anatomically special, that is, different from the V1 of other taxa and other cortical areas. Does other evidence support this observation?

Primate primary visual cortex differs structurally, functionally, and genetically from other cortical areas and, notably, from primary visual cortex in nonprimates. In nonprimates, primary visual cortex can be considered to have the standard six layers, but primates clearly have additional layers (24, 25). According to the most widely used lamination scheme, in primates, layer 3 is subdivided into 3A and 3B, and layer 4 is replaced by sublayers 4A, 4B, 4Cα, and 4Cβ.

In addition, there is evidence for corresponding functional differences between primate and nonprimate visual areas. For example, in cats, orientation selectivity of V1 neurons arises in the projection of the lateral geniculate to cortex (26), whereas in primates, the orientation selectivity is produced in the cortical circuitry (27).

Last, molecular markers can identify specific neocortical layers across areas within a species and across species (28, 29). Monkey and human area 17 are, however, more different molecularly from other primate areas (even area 18), and from nonprimate V1 (30). This observation provides a molecular correlate for the unique character of primate primary visual cortex that supports anatomical and function differences described above.

Evaluation of Methods for Quantitative Studies of Cell Number and Density. In the past three decades, researchers have mainly used two methods for studying cell numbers and densities: stereology and, more recently, the isotropic fractionator. Each method is best suited for particular types of problems. Modern stereology has excellent spatial resolution that extends to submicroscopic scales and is used for a wide variety of measurements that involve unbiased inferences about 3D structures from 2D sections through them. The isotropic fractionator method has lower spatial resolution and is designed especially for counting the number of cells in large populations. Both methods, in principle, are accurate, but have significant limitations in practice such as sensitivity to the idiosyncrasies of different experimenters or laboratories and are the cause of much disagreement. We consider the most important limitations in turn.

Critique of Stereology. A typical problem for which stereology should be well suited is the determination of average neuronal density in the visual cortex of macaque. Three studies of neuronal volume density (average number of neurons in a cubic millimeter of macaque V1) that found values of 119,900, 247,050, and 422,149 neurons/mm^3 illustrate the problem. The first paper (12) is an important and widely cited study on laminar volume densities in V1, the second (31) examines changes in neuron number (or lack thereof) with age, and the third (32) is part of a project to investigate the question of concerted vs. mosaic brain evolution by comparing scaling laws for visual cortex and hippocampus in carnivores and primates. How could determining the number of neurons per cubic millimeter differ so much in three studies?

It is impossible to know which values are correct and why they differ so much, but we can identify a general class of reasons. The first study (the source of the lowest value for monkey V1 in Fig. 3) was carried out before modern stereology was initiated (33) and techniques became standardized. The next two studies are, however, recent and used current methods of stereology that are efficient and unbiased.

Aside from random fluctuations in values and differences between brains (34), modern stereological procedures are guaranteed to be accurate (i.e., error magnitudes can be estimated). This guarantee only holds if the assumptions made by the technique are valid, but, in practice, they may not be. For example, the method assumes that random regions of interest are selected, but other constraints may restrict the possible selections. Accurate counts of cells under a square millimeter of surface require that the counting frame be normal to the surface, but curvature of the brain and the plane of section may mean that only certain counting frames are suitable. As another example, if frozen sections are used, the optical fractionator method assumes that the investigator knows the counting frame thickness in the *z* direction (the direction normal to the section surface), but nonuniform shrinkage in the *z* direction (9, 35) may cause this assumption to be incorrect and thus give cell volume densities that are over- or underestimates (36).

In summary, not all assumptions made by modern stereology methods are, in practice, exactly fulfilled, and the error magnitude associated with the violation of these assumptions cannot be estimated.

Critique of the isotropic fractionator method. Several decades were required for stereology to attain its current level of accuracy, and presumably the isotropic fractionator method (37) is still evolving. For example, only recently was a direct comparison made between two approaches to the isotropic fractionator and modern unbiased stereology (13), and this study—which demonstrated generally good agreement between the three methods—used some modifications of the isotropic fractionator method that were not used in earlier work.

The main difficulty with the current use of the isotropic fractionator is that the accuracy of the method for a given application cannot be estimated. The first step in the procedure is to homogenize a brain sample of known volume and to collect the resulting cell nuclei. Homogenization, however, can produce two sources of error (2): cell clumps and destruction of nuclei, both of which cause an underestimate of the true cell number. The magnitude of this error varies with the details of how the disaggregation was carried out, and it is impossible to estimate the error magnitude without some independent way of counting all of the cells (like DNA extraction and quantification of parallel samples).

The second difficulty lies in determining the fraction of all cells that are neurons. The current procedure is to label and count neurons with neuronal nuclei (NeuN) and then to get the number of glia by subtracting the number of neurons from the total. The fraction of cells that are neurons, as determined with NeuN alone, is uncertain because immunostaining is not all-or-none, there is no check by directly staining glia (we are not aware of a nuclear glial antibody), glia and neurons may not survive the disaggregation step equally, and the error magnitude in counting total cells (see above) is unknown. This issue is also relevant for stereology studies (38) that use NeuN for getting neuron and glia estimates.

A third difficulty specific to validating Rockel et al.'s observations is that the optical fractionator and other methods that count over large volumes are ill suited for identifying average neuronal surface densities in areas where the thicknesses or volume densities vary (39). According to Rockel et al., the number of neurons under a square millimeter is constant, irrespective of cortical thickness. Thus, volume densities cannot be used as a proxy unless thickness estimates are available for each volume density estimate. Second, counting cells over large volumes is problematic as the average of many surface density counts might not be the same as the overall average (38, 39).

Until the isotropic fractionator method can be modified so that error magnitudes can be estimated, the results produced will be subject to criticism.

In summary, because both techniques can give erroneous results, the only option is to make use of the observation that different laboratories make different errors and to rely on the weight of the evidence from the agreement of different studies. At this point, we would argue that the conclusions of Rockel et al. have not been disproved and that many more studies may be required to discover how their conclusions can fit into the larger question of cortical uniformity across areas and taxa.

Experimental Procedures

Histological Procedures. Histological procedures have been described previously (2). Specific characteristics of specimens used are detailed in Table S1. The storage of all specimens except A9 are described in ref. 2. A9 was stored in 0.01 M PBS and 0.05% sodium azide.

Data Collection. Data collection has been previously described in detail (2). The visual regions were outlined based on standard atlases and primary literature (40–43) with Neurolucida (version 10.01; MBF Bioscience) at low magnification (2× and 4× objectives). Examples of marked regions for each of the species are shown in Fig. S1. Counting columns were chosen as outlined in ref. 2, and neurons and glia were counted with standard unbiased stereology techniques (44–46) in Nissl-stained sections at 100× oil magnification, with no more than two counting frames per section. Neurons were differentiated from glia on the basis of size (bigger) and morphology (distinctive shape and processes extending out) of the cell and by the presence of a nucleolus. Glia were also more punctate. A few cells (less than 10%) were hard to distinguish and were labeled as unknown and not included in the neuronal count. Approximately 50–100 objects of interest were counted in each 3D column and eight columns per visual region. The total number of neurons counted ranged from 400 to 800 neurons per specimen for each region. We counted all of the neurons and glia in our column from the pial surface to the white matter without the use of guard zones. A detailed discussion of guard zone use as it pertains to stereological methods and data collection for frozen sections was reported in Carlo and Stevens (9).

Thionin Staining. The tissue was defatted with 100% (vol/vol) ethanol:chloroform (1:1) overnight, rehydrated in a decreasing alchohol (with DI H_2O) series (100%, 95%, 70%, 50%), treated with DI H_2O, thionin stain, followed by DI H_2O, an increasing alcohol series (50%, 70%, 95%, 95%, 100%, 100%), Xylenes I, and Xylenes II, and then coverslipped. The tissue was dipped four to five times in each of the solutions for 1 min except for the thionin stain (1–2 min) and Xylenes II (1 h). The thionin stain was prepared by first gently heating 1,428 mL DI H_2O, 54 mL 1 M NaoH, and 18 mL glacial acetic acid until the solution was steaming. Then, 3.75 g thionin was added, and the solution was boiled gently for 45 min, cooled, filtered, and used for staining.

Calculations, Statistical Analyses, and Controls for Systematic Errors. This information has been described previously (2).

ACKNOWLEDGMENTS. We thank Anita Disney for providing monkey sections and advice and Junko Ogawa for help with imaging. We also thank the National Science Foundation (NSF) directorate of Mathematical and Physical Sciences for their support through the 2014 NSF Early-Concept Grants for Exploratory Research (NSF PHY-1444273) award.

1. Rockel AJ, Hiorns RW, Powell TPS (1980) The basic uniformity in structure of the neocortex. *Brain* 103(2):221–244.
2. Carlo CN, Stevens CF (2013) Structural uniformity of neocortex, revisited. *Proc Natl Acad Sci USA* 110(4):1488–1493.
3. de Sousa AA, Proulx MJ (2014) What can volumes reveal about human brain evolution? A framework for bridging behavioral, histometric, and volumetric perspectives. *Front Neuroanat* 8:51.
4. Clifford CW, Ibbotson MR (2002) Fundamental mechanisms of visual motion detection: Models, cells and functions. *Prog Neurobiol* 68(6):409–437.
5. Blasdel GG (1992) Orientation selectivity, preference, and continuity in monkey striate cortex. *J Neurosci* 12(8):3139–3161.
6. Bonhoeffer T, Grinvald A (1991) Iso-orientation domains in cat visual cortex are arranged in pinwheel-like patterns. *Nature* 353(6343):429–431.
7. Stevens CF (2001) An evolutionary scaling law for the primate visual system and its basis in cortical function. *Nature* 411(6834):193–195.
8. Veilleux CC, Kirk EC (2014) Visual acuity in mammals: Effects of eye size and ecology. *Brain Behav Evol* 83(1):43–53.
9. Carlo CN, Stevens CF (2011) Analysis of differential shrinkage in frozen brain sections and its implications for the use of guard zones in stereology. *J Comp Neurol* 519(14):2803–2810.
10. Schuz A, Palm Gu (1989) Density of neurons and synapses in the cerebral cortex of the mouse. *J Comp Neurol* 286(4):442–455.
11. Gabbott PL, Stewart MG (1987) Distribution of neurons and glia in the visual cortex (area 17) of the adult albino rat: A quantitative description. *Neuroscience* 21(3):833–845.
12. O'Kusky J, Colonnier M (1982) A laminar analysis of the number of neurons, glia, and synapses in the visual cortex (area 17) of adult macaque monkeys. *J Comp Neurol* 210(3):278–290.
13. Miller DJ, Balaram P, Young NA, Kaas JH (2014) Three counting methods agree on cell and neuron number in chimpanzee primary visual cortex. *Front Neuroanat* 8:36.
14. Beaulieu C, Colonnier M (1983) The number of neurons in the different laminae of the binocular and monocular regions of area 17 in the cat, Canada. *J Comp Neurol* 217(3):337–344.
15. Mayhew TM, Mwamengele GL, Dantzer V (1996) Stereological and allometric studies on mammalian cerebral cortex with implications for medical brain imaging. *J Anat* 189(Pt 1):177–184.
16. Kaskan PM, et al. (2005) Peripheral variability and central constancy in mammalian visual system evolution. *Proc Biol Sci* 272(1558):91–100.
17. Yellot JI, Wandell B, Cornsweet TN (1984) *The Beginnings of Visual Perception: The Retinal Image and Its Initial Encoding. Handbook of Physiology* (Americal Physiological Society, Bethesda, MD), pp 257–316.
18. Swindale NV, Matsubara JA, Cynader MS (1987) Surface organization of orientation and direction selectivity in cat area 18. *J Neurosci* 7(5):1414–1427.
19. Stevens CF (2015) Novel neural circuit mechanism for visual edge detection. *Proc Natl Acad Sci USA* 112(3):875–880.
20. Xu X, et al. (2004) Functional organization of visual cortex in the owl monkey. *J Neurosci* 24(28):6237–6247.
21. Blasdel GG, Salama G (1986) Voltage-sensitive dyes reveal a modular organization in monkey striate cortex. *Nature* 321(6070):579–585.
22. Rao SC, Toth LJ, Sur M (1997) Optically imaged maps of orientation preference in primary visual cortex of cats and ferrets. *J Comp Neurol* 387(3):358–370.
23. Law MI, Zahs KR, Stryker MP (1988) Organization of primary visual cortex (area 17) in the ferret. *J Comp Neurol* 278(2):157–180.
24. Lund JS, Henry GH, MacQueen CL, Harvey AR (1979) Anatomical organization of the primary visual cortex (area 17) of the cat. A comparison with area 17 of the macaque monkey. *J Comp Neurol* 184(4):599–618.
25. Callaway EM (1998) Local circuits in primary visual cortex of the macaque monkey. *Annu Rev Neurosci* 21:47–74.
26. Hubel DH, Wiesel TN (1962) Receptive fields, binocular interaction and functional architecture in the cat's visual cortex. *J Physiol* 160:106–154.
27. Hubel DH, Wiesel TN (1968) Receptive fields and functional architecture of monkey striate cortex. *J Physiol* 195(1):215–243.
28. Belgard TG, et al. (2011) A transcriptomic atlas of mouse neocortical layers. *Neuron* 71(4):605–616.
29. Dugas-Ford J, Rowell JJ, Ragsdale CW (2012) Cell-type homologies and the origins of the neocortex. *Proc Natl Acad Sci USA* 109(42):16974–16979.
30. Bernard A, et al. (2012) Transcriptional architecture of the primate neocortex. *Neuron* 73(6):1083–1099.
31. Giannaris EL, Rosene DL (2012) A stereological study of the numbers of neurons and glia in the primary visual cortex across the lifespan of male and female rhesus monkeys. *J Comp Neurol* 520(15):3492–3508.
32. Lewitus E, Kelava I, Kalinka AT, Tomancak P, Huttner WB (2013) An adaptive threshold in mammalian neocortical evolution. arXiv:13045412.
33. Sterio DC (1984) The unbiased estimation of number and sizes of arbitrary particles using the disector. *J Microsc* 134(Pt 2):127–136.
34. Andrews TJ, Halpern SD, Purves D (1997) Correlated size variations in human visual cortex, lateral geniculate nucleus, and optic tract. *J Neurosci* 17(8):2859–2868.
35. Noori HR, Fornal CA (2011) The appropriateness of unbiased optical fractionators to assess cell proliferation in the adult hippocampus. *Front Neurosci* 5:140.
36. Charvet CJ, Cahalane DJ, Finlay (2015) Systematic, cross-cortex variation in neuron numbers in rodents and primates. *Cereb Cortex* 25(1):147–160.
37. Herculano-Houzel S, Lent R (2005) Isotropic fractionator: A simple, rapid method for the quantification of total cell and neuron numbers in the brain. *J Neurosci* 25(10):2518–2521.
38. Meyer HS, et al. (2013) Cellular organization of cortical barrel columns is whisker-specific. *Proc Natl Acad Sci USA* 110(47):19113–19118.
39. Herculano-Houzel S, Watson C, Paxinos G (2013) Distribution of neurons in functional areas of the mouse cerebral cortex reveals quantitatively different cortical zones. *Front Neuroanat* 7:35.
40. Paxinos G, Huang X-F, Toga AW (1999) The rhesus monkey brain in stereotaxic coordinates. (Academic, New York).
41. Paxinos G, Watson C (2006) *The Rat Brain in Stereotaxic Coordinates* (Academic Press, New York).
42. Payne B, Peters A (2001) *The Cat Primary Visual Cortex* (Academic Press, New York).
43. Paxinos G, Franklin KB (2004) *The Mouse Brain in Stereotaxic Coordinates* (Gulf Professional Publishing, Houston).
44. West MJ, Gundersen HJG (1990) Unbiased stereological estimation of the number of neurons in the human hippocampus. *J Comp Neurol* 296(1):1–22.
45. West MJ, Slomianka L, Gundersen HJG (1991) Unbiased stereological estimation of the total number of neurons in thesubdivisions of the rat hippocampus using the optical fractionator. *Anat Rec* 231(4):482–497.

46. Howard V, Reed M (2004) *Unbiased Stereology: Three-Dimensional Measurement in Microscopy* (Garland Science New York).
47. Hendry SH, Schwark HD, Jones EG, Yan J (1987) Numbers and proportions of GABA-immunoreactive neurons in different areas of monkey cerebral cortex. *J Neurosci* 7(5): 1503–1519.
48. Skoglund TS, Pascher R, Berthold C-H (1996) Heterogeneity in the columnar number of neurons in different neocortical areas in the rat. *Neurosci Lett* 208(2):97–100.
49. DeFelipe J, Alonso-Nanclares L, Arellano JI (2002) Microstructure of the neocortex: Comparative aspects. *J Neurocytol* 31(3-5):299–316.
50. Van Essen DC, Maunsell JH (1980) Two-dimensional maps of the cerebral cortex. *J Comp Neurol* 191(2):255–281.
51. Van Essen DC, Newsome WT, Maunsell JH (1984) The visual field representation in striate cortex of the macaque monkey: Asymmetries, anisotropies, and individual variability. *Vision Res* 24(5):429–448.
52. Condo GJ, Casagrande VA (1990) Organization of cytochrome oxidase staining in the visual cortex of nocturnal primates (Galago crassicaudatus and Galago senegalensis): I. Adult patterns. *J Comp Neurol* 293(4):632–645.
53. Van Hooser SD, Heimel JAF, Chung S, Nelson SB, Toth LJ (2005) Orientation selectivity without orientation maps in visual cortex of a highly visual mammal. *J Neurosci* 25(1):19–28.
54. Tyler CJ, et al. (1998) Anatomical comparison of the macaque and marsupial visual cortex: common features that may reflect retention of essential cortical elements. *J Comp Neurol* 400(4):449–468.